Double electron capture between an α particle and a helium atom in the presence of an intense laser field

Shu-Min Li
China Center of Advanced Science and Technology (World Laboratory), P.O. Box 8730, Beijing 100 080, People's Republic of China and Department of Modern Physics, University of Science and Technology of China, P.O. Box 4, Hefei, Anhui 230 027, People's Republic of China

Yan-Gang Miao
China Center of Advanced Science and Technology (World Laboratory), P.O. Box 8730, Beijing 100 080, People's Republic of China and Department of Physics, Xiamen University, Xiamen 361 005, People's Republic of China

Zi-Fang Zhou, Ji Chen, and Yao-Yang Liu
Department of Modern Physics, University of Science and Technology of China, P.O. Box 4, Hefei, Anhui 230 027, People's Republic of China

(Received 8 July 1997)

In the first Born approximation, the symmetrical double-electron-capture collision between an α particle and a helium atom in the presence of an intense laser field is studied. The capture cross section is promoted considerably and is an increasing function of the ratio of the laser amplitude to frequency. With increasing impact energy, the dressing modification becomes notable. [S1050-2947(98)01204-9]

PACS number(s): 34.50.Rk, 34.70.+e, 32.80.Wr, 34.90.+q

I. INTRODUCTION

With the development of laser technology, the study of the dressing effect on atomic systems has long been an active area of research in physics, both when dealing with isolated atoms and when the attention is focused on many-particle processes [electron- (or positron-) atom and atom- (ion-) atom collisions] [1,2]. In past decades, interests has mainly focused on photon-atom interactions and collisional effects on light emission [2]. The laser modification on low-energy atom-atom (ion) collisions in a relatively weak field were extensively studied [3–6], where the two-state model and quasimolecular approximation were generally employed. For intense field-assisted electron- and positron-atom scattering, some calculation based on the first Born approximation (FBA) are made [7–10].

In this article, we address an investigation into the double-electron-capture collision in the presence of an intense laser background. We begin with the simplest collision of this kind,

$$\mathrm{He}^{2+}\mathrm{He}(1s) \xrightarrow[\text{Laser}]{} \mathrm{He}(1s)+\mathrm{He}^{2+}, \tag{1.1}$$

and for less complexity assume that the laser is a linearly polarized classical electromagnetic field. The vector potential is

$$\vec{A}=\vec{A}_0 \cos \omega t=\frac{c}{\omega} \vec{\mathcal{E}}_0 \cos \omega t, \tag{1.2}$$

where $\vec{\mathcal{E}}_0$ is the electric vector of the field. The magnitude of this vector is far less than an atomic unit (1 a.u. of field strength $\approx 5.14\times 10^9$ V cm^{-1}), but intense enough by laboratory standards. This ensures that a perturbative treatment of the field-atom interaction is applicable. Atomic units ($e=m=\hbar=1$) are employed unless otherwise stated.

II. THEORY

We examine the collision of Eq. (1.1) when the helium target is set in its dressed ground state. The projectile, target nucleus, and electrons are labeled P, N, and e_1 and e_2, respectively. The coordinate system is illustrated in Fig. 1.

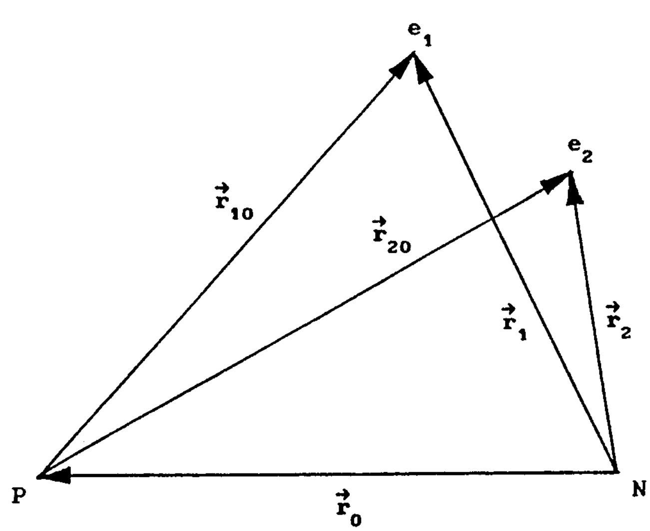

FIG. 1. Coordinate system for laser-assisted He^{2+}-He double electron capture.

The channel Hamiltonians and channel interactions for initial and final states may be written as

$$H_I=-\frac{1}{2\mu_I}\nabla^2_{\vec{R}}-\frac{1}{2}\left(\nabla_{\vec{r}_1}+\frac{i}{c}\vec{A}\right)^2-\frac{1}{2}\left(\nabla_{\vec{r}_2}+\frac{i}{c}\vec{A}\right)^2-\frac{Z_N}{r_1}-\frac{Z_N}{r_2}+\frac{1}{r_{12}}, \tag{2.1}$$

$$V_I=\frac{Z_PZ_N}{r_0}-\frac{Z_P}{r_{10}}-\frac{Z_P}{r_{20}}, \tag{2.2}$$

$$H_F=-\frac{1}{2\mu_F}\nabla^2_{\vec{R}'}-\frac{1}{2}\left(\nabla_{\vec{r}_{10}}+\frac{i}{c}\vec{A}\right)^2-\frac{1}{2}\left(\nabla_{\vec{r}_{20}}+\frac{i}{c}\vec{A}\right)^2-\frac{Z_P}{r_{10}}-\frac{Z_P}{r_{20}}+\frac{1}{r_{12}}, \tag{2.3}$$

$$V_F=\frac{Z_PZ_N}{r_0}-\frac{Z_N}{r_1}-\frac{Z_N}{r_2}, \tag{2.4}$$

where $Z_P=Z_N=2$ denote the charges of the projectile and target nucleus, $\mu_I=M_P(M_N+2)/(M_P+M_N+2)=\mu_F$ the reduced masses of initial and final states ($M_P=M_N$ are the masses of projectile and target nucleus), and $\vec{R}=\vec{r}_0-(\vec{r}_1+\vec{r}_2)/(M_N+2)$ and $\vec{R}'=(M_P\vec{r}_0+\vec{r}_1+\vec{r}_2)/(M_P+2)$ the relative coordinates between both colliders in the initial and final states.

In the FBA, the S-matrix element associated with the laser modified ground-state-to-ground-state double electron capture is

$$S^{B_1}=-i\int_{-\infty}^{\infty}dt\langle\chi_F(\vec{R}',t)\psi_0^{\mathrm{He}}(\vec{r}_{10},\vec{r}_{20},t)\times|V_I|\chi_I(\vec{R},t)\psi_0^{\mathrm{He}}(\vec{r}_1,\vec{r}_2,t)\rangle, \tag{2.5}$$

where χ_I and χ_F are the incoming and outgoing plane waves (the dressing on them has been omitted). ψ_0^{He} is the perturbative wave function for the dressed ground state of helium in the soft photon approximation [11],

$$\psi_0^{\mathrm{He}}(\vec{r}_1,\vec{r}_2,t)=e^{-iW_0^{\mathrm{He}}t}[\phi_0^{\mathrm{He}}(\vec{r}_1,\vec{r}_2)-\cos\,\omega t\,\tilde{\phi}_0^{\mathrm{He}}(\vec{r}_1,\vec{r}_2)], \tag{2.6}$$

with

$$\tilde{\phi}_0^{\mathrm{He}}(\vec{r}_1,\vec{r}_2)=-\frac{1}{\omega_{\mathrm{He}}\omega}\vec{\mathcal{E}}_0\cdot\sum_{j=1}^{2}\nabla_{\vec{r}_j}\phi_0^{\mathrm{He}}(\vec{r}_1,\vec{r}_2), \tag{2.7}$$

where $\omega_{\mathrm{He}}=1.15$ a.u. is the average excitation energy of helium. In Eqs. (2.6) and (2.7), we choose state vector $\phi_0^{\mathrm{He}}(\vec{r}_1,\vec{r}_2)$ as the Hartree-Fock wave function of helium [12],

$$\phi_0^{\mathrm{He}}(\vec{r}_1,\vec{r}_2)=\phi_0(\vec{r}_1)\phi_0(\vec{r}_2), \tag{2.8}$$

with

$$\phi_0(\vec{r})=\frac{1}{\sqrt{4\pi}}\sum_{i=1}^{2}C_ie^{-\alpha_ir}, \tag{2.9}$$

in which $C_1=2.605\,05$, $C_2=2.081\,44$, $\alpha_1=1.41$, and $\alpha_2=2.61$.

Substituting Eq. (2.6) into Eq. (2.5), neglecting the higher-order dressing terms, and then working out the time integration, we gain

$$S^{B_1}=(2\pi)^{-1}i\sum_{l=-1}^{+1}f_l^{B_1}\delta(E_F-E_I+l\omega), \tag{2.10}$$

in which,

$$\begin{aligned}f_0^{B_1}&=-\frac{\mu_F}{2\pi}\int d\vec{R}\,d\vec{r}_1d\vec{r}_2e^{-i\vec{k}_F\cdot\vec{R}'}e^{i\vec{k}_I\cdot\vec{R}}\phi_0^{\mathrm{He}*}(\vec{r}_{10},\vec{r}_{20})V_I\phi_0^{\mathrm{He}}(\vec{r}_1,\vec{r}_2)\\&=-\frac{\mu_F}{2\pi}\int d\vec{r}_0d\vec{r}_1d\vec{r}_2e^{-i\vec{q}_0\cdot\vec{r}_0}e^{-i\vec{q}_1\cdot\vec{r}_1}e^{-i\vec{q}_2\cdot\vec{r}_2}\phi_0^{\mathrm{He}*}(\vec{r}_{10},\vec{r}_{20})V_I\phi_0^{\mathrm{He}}(\vec{r}_1,\vec{r}_2),\end{aligned} \tag{2.11}$$

$$\begin{aligned}f_{\pm1}^{B_1}&=-\frac{\mu_F}{2\pi}\int d\vec{R}\,d\vec{r}_1d\vec{r}_2e^{-i\vec{k}_F\cdot\vec{R}'}e^{i\vec{k}_I\cdot\vec{R}}[\tilde{\phi}_0^{\mathrm{He}*}(\vec{r}_{10},\vec{r}_{20})V_I\phi_0^{\mathrm{He}}(\vec{r}_1,\vec{r}_2)+\phi_0^{\mathrm{He}*}(\vec{r}_{10},\vec{r}_{20})V_I\tilde{\phi}_0^{\mathrm{He}}(\vec{r}_1,\vec{r}_2)]\\&=-\frac{\mu_F}{2\pi}\int d\vec{r}_0d\vec{r}_1d\vec{r}_2e^{-i\vec{q}_0\cdot\vec{r}_0}e^{-i\vec{q}_1\cdot\vec{r}_1}e^{-i\vec{q}_2\cdot\vec{r}_2}[\tilde{\phi}_0^{\mathrm{He}*}(\vec{r}_{10},\vec{r}_{20})V_I\phi_0^{\mathrm{He}}(\vec{r}_1,\vec{r}_2)+\phi_0^{\mathrm{He}*}(\vec{r}_{10},\vec{r}_{20})V_I\tilde{\phi}_0^{\mathrm{He}}(\vec{r}_1,\vec{r}_2)],\end{aligned} \tag{2.12}$$

where $\vec{q}_0=\vec{k}_FM_P/(M_P+2)-\vec{k}_I$ and $\vec{q}_1=\vec{q}_2=\vec{k}_F/(M_P+2)+\vec{k}_I/(M_N+2)$ are the momentum transfers of the projectile and both electrons, respectively. Using the Feynman parametric integration technique, we may reduce the ninefold integration of Eq. (2.11) to

$$f_0^{B_1}=-\frac{\mu_F}{2}\sum_{i,j,m,n}C_iC_jC_mC_nI_{ijmn}, \tag{2.13}$$

with

$$I_{ijmn}=\left(Z_PZ_N\frac{\partial}{\partial\alpha_i}-2Z_P\frac{\partial}{\partial\gamma}\right)\frac{\partial}{\partial\alpha_j}\frac{\partial}{\partial\beta_m}\frac{\partial}{\partial\beta_n}\mathcal{I}(\vec{q}_0,\gamma,\vec{q}_1,\alpha_i,\vec{q}_2,\alpha_j,\beta_m,\beta_n), \tag{2.14}$$

where

$$\mathcal{I}(\vec{q}_0,\gamma,\vec{q}_1,\alpha_i,\vec{q}_2,\alpha_j,\beta_m,\beta_n)=\frac{1}{16\pi^3}\int d\vec{r}_0d\vec{r}_1d\vec{r}_2\frac{e^{-i\vec{q}_0\cdot\vec{r}_0-\gamma r_0}}{r_0}\frac{e^{-i\vec{q}_1\cdot\vec{r}_1-\alpha_ir_1}}{r_1}\frac{e^{-i\vec{q}_2\cdot\vec{r}_2-\alpha_jr_2}}{r_2}\frac{e^{-\beta_mr_{10}}}{r_{10}}\frac{e^{-\beta_nr_{20}}}{r_{20}}$$
$$=\int_0^1d\xi\int_0^1d\eta\frac{1}{\rho_1\rho_2[(\rho_1+\rho_2+\gamma)^2+q^2]}, \tag{2.15}$$

in which

$$\vec{q}=\vec{q}_0+\vec{q}_1\xi+\vec{q}_2\eta, \tag{2.16}$$

$$\rho_1=[\beta_m^2+(q_1^2+\alpha_i^2-\beta_m^2)\xi-q_1^2\xi^2]^{1/2}, \tag{2.17}$$

$$\rho_2=[\beta_n^2+(q_2^2+\alpha_j^2-\beta_n^2)\eta-q_2^2\eta^2]^{1/2}. \tag{2.18}$$

The reduction of Eq. (2.15) appears in the Appendix. Similarly, we may reduce Eq. (2.12) to

$$f_{\pm1}^{B_1}=-\frac{\mu_F}{2}\sum_{i,j,m,n}C_iC_jC_mC_n\tilde{I}_{ijmn}, \tag{2.19}$$

where

$$\tilde{I}_{ijmn}=\frac{\mathcal{E}_0}{\omega}\left\{\left[\frac{\alpha_i}{\omega_{\mathrm{He}}}\frac{\partial}{\partial q_{1\varepsilon}}\left(Z_PZ_N\frac{\partial}{\partial\alpha_i}-Z_P\frac{\partial}{\partial\gamma}\right)\frac{\partial}{\partial\beta_m}\frac{\partial}{\partial\beta_n}\right.\right.$$
$$-\frac{\beta_m}{\omega_{\mathrm{He}}}\left(\frac{\partial}{\partial q_{1\varepsilon}}-\frac{\partial}{\partial q_{0\varepsilon}}\right)\left(Z_PZ_N\frac{\partial}{\partial\alpha_i}-2Z_P\frac{\partial}{\partial\gamma}\right)\left.\frac{\partial}{\partial\beta_n}\right]$$
$$\times\mathcal{I}(\vec{q}_0,\gamma,\vec{q}_1,\alpha_i,\vec{q}_2,\alpha_j,\beta_m,\beta_n)$$
$$+Z_P\frac{\alpha_i}{\omega_{\mathrm{He}}}\frac{\partial}{\partial q_{1\varepsilon}}\frac{\partial}{\partial\gamma}\frac{\partial}{\partial\alpha_j}\frac{\partial}{\partial\beta_m}\frac{\partial}{\partial\beta_n}$$
$$\left.\times\int_{\alpha_i}^{\infty}d\alpha_i'\mathcal{I}(\vec{q}_0,\gamma,\vec{q}_1,\alpha_i',\vec{q}_2,\alpha_j,\beta_m,\beta_n)\right\}. \tag{2.20}$$

The laser-modified double-electron-capture cross section is a sum of all cross sections with a definite number of photons exchanged,

$$\frac{d\sigma^{B_1}}{d\Omega}=\sum_{l=-1}^{+1}\frac{k_F}{k_I}|f_l^{B_1}|^2. \tag{2.21}$$

In carrying out the numerical calculation of Eqs. (2.14) and (2.20), we first used MATHEMATICA to derive the parametric differentiation of the integrands, and then transferred them into FORTRAN programs. The twofold and threefold numerical integrations are finally completed in FORTRAN.

III. RESULTS AND DISCUSSION

In Fig. 2 the differential cross sections for laser-modified double electron capture in the center-of-mass system are displayed. We plot the cross sections for polarization geometries of $\vec{\mathcal{E}}_0\parallel\vec{k}_I$ and $\vec{\mathcal{E}}_0\perp\vec{k}_I$, as well as the result for laser absence. For both geometries, the double-capture cross sections are promoted with application of the electric field. Such collisional behavior can be understood by the ''relaxation effect'' of dressing on each atom. When the laser is present, the fast Coulomb binding of the target nucleus on electrons is relaxed due to the laser polarization, which is preferable to electron capture at the impact energy and the field strength considered. The result for an extremely small scattering angle ($\theta\sim0°$) corresponds to the situation that the projectile does not ''penetrate'' into the electron clouds of the target. When the field polarization is set parallel to the incident direction, the velocity of electrons relative to the projectile is maximally changed, while for a perpendicular geometry the velocity change is smaller. The relative velocity is one of the decisive factors that affect the electron-capture probability; therefore, at small scattering angles, the double-electron-capture cross section for a parallel geometry is greater than

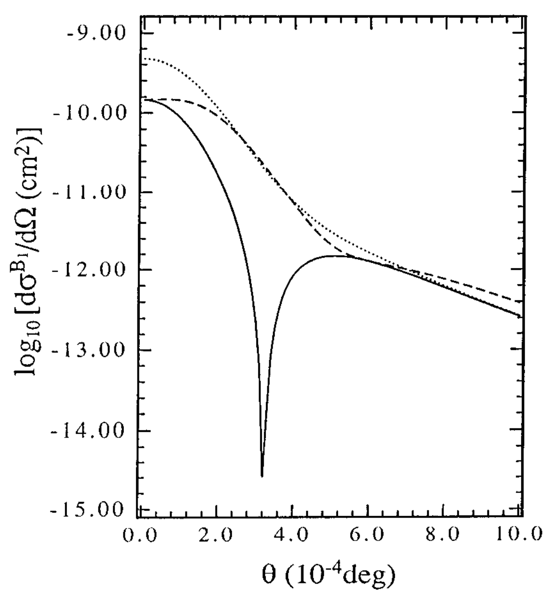

FIG. 2. Differential cross section for laser-assisted He^{2+}-He double electron capture from ground state to ground state in the center-of-mass system at the laboratory impact energy $E_L=400$ keV, field strength $\mathcal{E}_0=2.0\times10^8$ V cm^{-1}, and frequency $\hbar\omega=1.17$ eV. Solid line, cross section for laser absence; dotted line, laser-modified result for a parallel geometry $\vec{\mathcal{E}}_0\parallel\vec{k}_I$; dashed line, result for a perpendicular geometry $\vec{\mathcal{E}}_0\perp\vec{k}_I$.

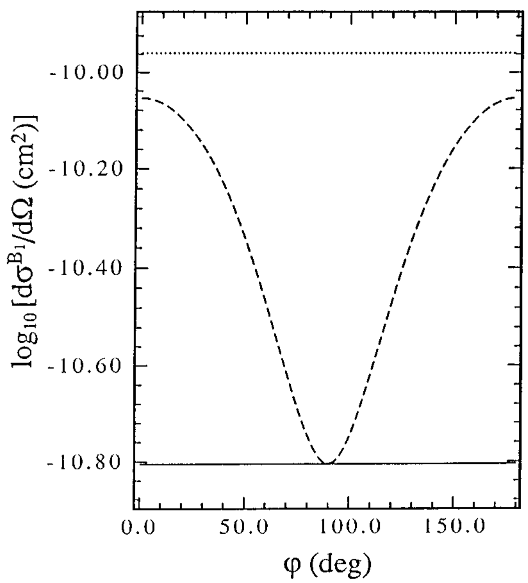

FIG. 3. Azimuth-angle dependence of the differential cross section at scattering angle $\theta = 1.0\times10^{-4}$ deg. Solid line, result for laser absence; dotted line, result for $\vec{\mathcal{E}}_0 \| \vec{k}_I$; dashed line, result for $\vec{\mathcal{E}}_0 \perp \vec{k}_I$.

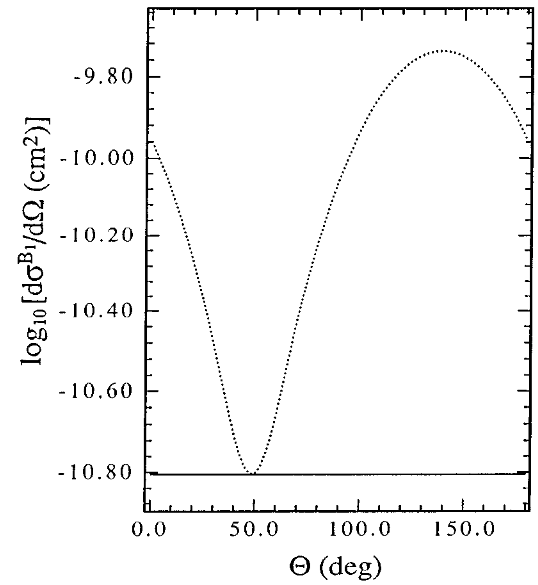

FIG. 5. Polarization direction dependence of differential cross section at $E_L = 400$ keV, $\mathcal{E}_0 = 2.0\times10^8$ V cm^{-1}, $\hbar\omega = 1.17$ eV, $\theta = 1.0\times10^{-4}$ deg, and $\varphi = 0°$. Solid line, result for laser absence; dotted line, laser-modified result.

that for a perpendicular geometry.

In Fig. 3 we give the azimuth angle (the angle between the polarization plane $\vec{k}_I \times \vec{\mathcal{E}}_0$ and the scattering plane $\vec{k}_I \times \vec{k}_F$) dependence for a perpendicular geometry. The theoretical result shows that when $\vec{k}_F$ is set in the polarization plane, the cross-section modification is maximum. When $\vec{k}_F$ deviates from the polarization plane, the laser modification decreases; at $\varphi = 90°$, the modification nearly disappears.

The resulting dependence on laser dynamic parameters is presented in Figs. 4 and 5. Figure 4 indicates that in the perturbative field range, the laser promotions on the cross section are mono-increasing functions of $\mathcal{E}_0/\omega$. The stronger the field, the greater the cross-section promotion; the lower the field frequency, the more the target is continuously polarized in a definite direction and thus the greater the promotion that leads to. This is easy to comprehend from Eq. (2.7). Figure 5 shows that with the polarization angle increasing (we have assumed that the scattering direction is

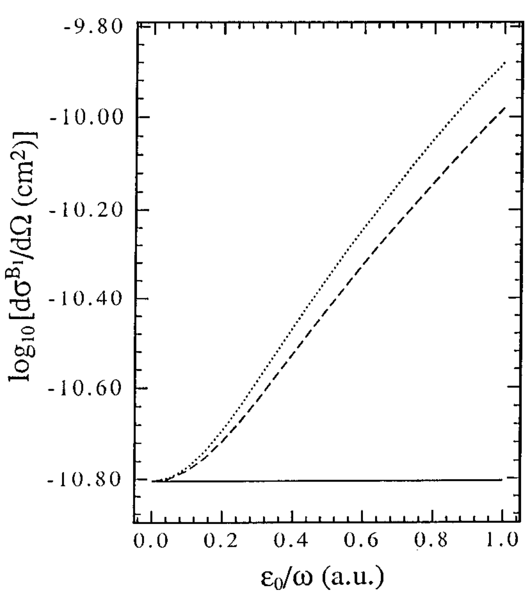

FIG. 4. Differential cross sections as functions of $\mathcal{E}_0/\omega$ for $E_L = 400$ keV, $\theta = 1.0\times10^{-4}$ deg, and $\varphi = 0°$. Solid line, result for laser absence; dotted line, result for $\vec{\mathcal{E}}_0 \| \vec{k}_I$; dashed line, result for $\vec{\mathcal{E}}_0 \perp \vec{k}_I$.

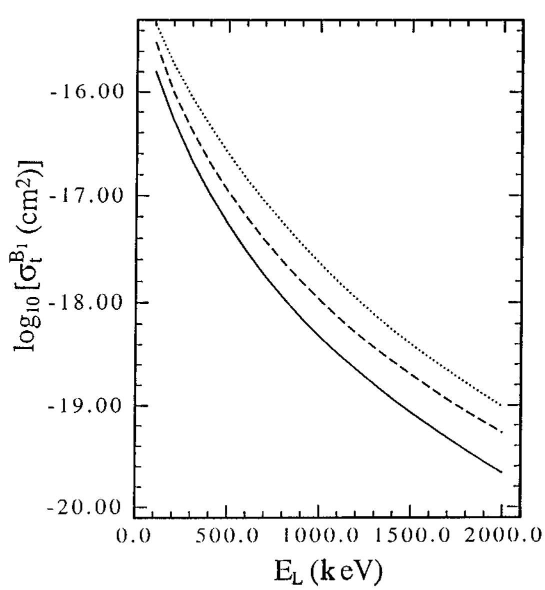

FIG. 6. Integral cross section for laser-assisted He^{2+}-He double electron capture at $\mathcal{E}_0 = 2.0\times10^8$ V cm^{-1} and $\hbar\omega = 1.17$ eV. Solid line, result for laser absence; dotted line, result for $\vec{\mathcal{E}}_0 \| \vec{k}_I$; dashed line, result for $\vec{\mathcal{E}}_0 \perp \vec{k}_I$.

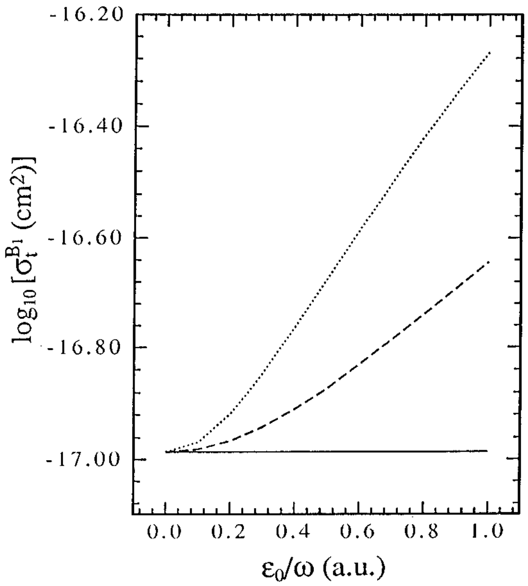

FIG. 7. Integral cross-section dependence on laser parameter $\mathcal{E}_0/\omega$ at $E_L = 400$ keV. Solid line, result for laser absence; dotted line, result for $\vec{\mathcal{E}}_0 \| \vec{k}_I$; dashed line, result for $\vec{\mathcal{E}}_0 \perp \vec{k}_I$.

set in the polarization plane), the laser-modified cross section first gradually drops to a minimum at $\Theta = 49°$ (the minimum is nearly the same as the result for laser absence), then increases in a large polarization angular range, at about $\Theta = 135°$ to its maximum, and then drops to a value that is the same as the result for $\Theta = 0°$.

In Fig. 6 we plot the total double-electron cross sections. For both geometries, the total cross section is promoted dramatically by the field. Because the angular distribution of the small scattering angle contributes the dominant part to the total cross section, the result for a parallel geometry is

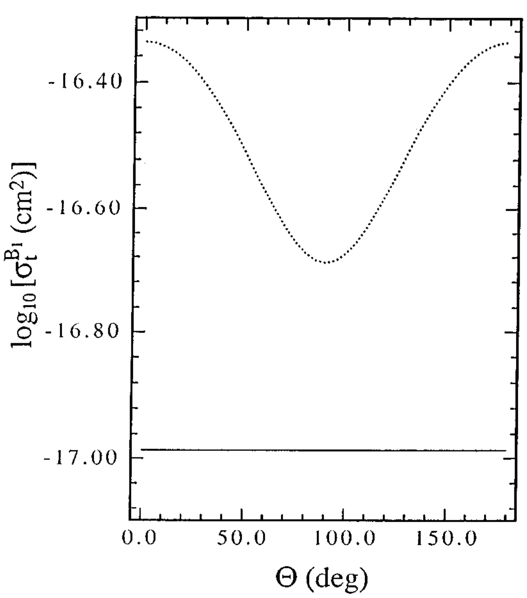

FIG. 8. Integral cross section dependence on polarization direction at $E_L = 400$ keV, $\mathcal{E}_0 = 2.0 \times 10^8$ V cm^{-1}, and $\hbar\omega = 1.17$ eV. Solid line, result for laser absence; dotted line, laser-modified result.

greater than that for perpendicular one.

The function relations between the total cross section and laser parameters are reported in Figs. 7 and 8. Figure 7 shows that the total-cross-section dependence on $\mathcal{E}_0/\omega$ is similar to the curve behavior of Fig. 4, except that the difference between both geometries is much more notable. In Fig. 8 the total-cross-section dependence on the polarization cross section is almost symmetric. At $\Theta = 0°$ and 180° (i.e., the parallel geometry) the laser promotion is at its maximum; at $\Theta = 90°$ (perpendicular geometry) it drops to its minimum.

IV. CONCLUSIONS

In summary, a theoretical prediction on laser modification to the symmetrical double electron capture between an α particle and a dressed helium atom has been made. Both differential and total cross sections are calculated. The cross-section dependence on laser strength, frequency, and polarization direction is discussed. Generally speaking, the cross section is greatly promoted by the laser. The promotion is

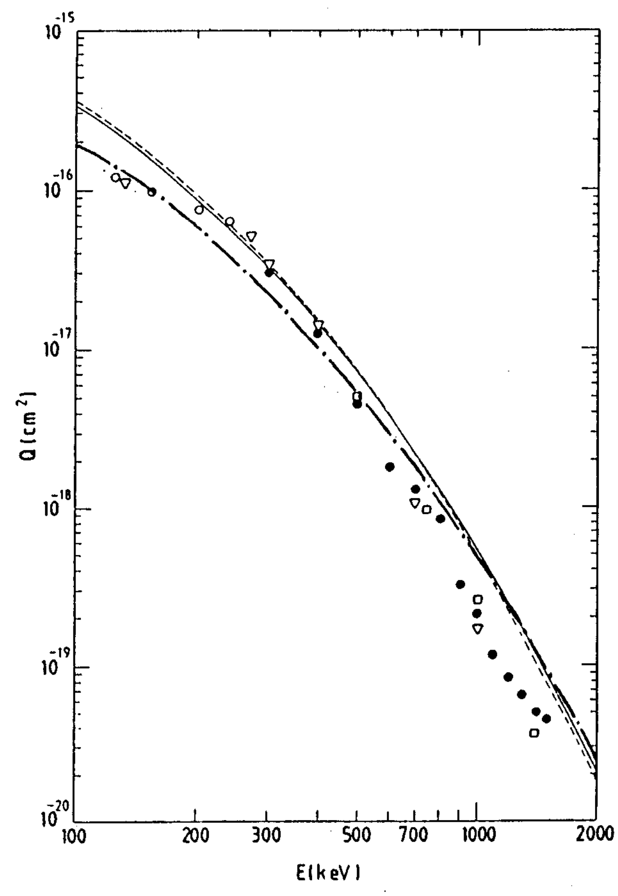

FIG. 9. Comparison of the FBA total cross section with other theoretical and experiment results for laser absence. Theoretical results ($1s^2$-$1s^2$ double electron capture only): dot-dashed line, present FBA calculation; dashed and solid lines, results by Belkić of correct first Born approximation (CB1) employing the completely uncorrelated Hylleraas orbitals for the cases without dynamic correlation [13] and with dynamic correlation [14]. Experimental data: open circles, Berkner *et al.* [15]; squares, McDaniel *et al.* [16]; closed circles, Pivovar *et al.* [17]; triangles, DuBois [18].

especially remarkable at high energy. Unlike other internuclear-interaction-dominated scattering processes, the charge-transfer collision is dominated by the nucleus-electron interaction at high energy instead of the internuclear one. Because a nucleus is at least 1840 times heavier than an electron, the dressing on nuclei is negligible. Thus at high energy the dressing-modified double-capture cross sections are much higher than the result for the laser-free capture cross section. The laser-free capture cross section of high energy in general is difficult to measure; the dressing modification suggests that we may detect some high-energy collisional parameters with the application of an intense laser background.

In the above discussion the electron correlation and its dressing modification are not considered. For this symmetric electron-capture collision, the interelectron Coulomb interaction is limited within the target helium or the newly formed helium in the final state. The Hartree-Fock wave function of Eq. (2.8) for helium does not include the electron correlation. If we believe that the correlation modification to the Hartree-Fock wave function is a small correction, according to Eq. (2.7), the corresponding dressing modification of it is a higher-order one. Therefore, the correlation effects on dressing and on the modified cross section are minor.

To our knowledge, there has been no report on laser modification to double-electron-capture collisions until now. To confirm the reliability of the FBA treatment on the double-electron-capture collision, in Fig. 9 we present a comparison of the FBA result for the absence of a laser with the theoretical results of the corrected first Born approximation [13,14] and some experimental results [15–18]. The figure shows that the FBA calculation for the undressed collision agrees with experiment in the energy range we considered.

ACKNOWLEDGMENTS

This work was supported by the Returned Student Foundation of Academia Sinica, the Start Foundation for Returned Student, and Chinese Research for Atomic and Molecular Data. Dr. Sandra J. Robinson of ORBIS read the manuscript and gave many helpful suggestions.

APPENDIX

In this appendix, we give the proof of Eq. (2.15). Substituting the Fourier transformations

$$\frac{e^{-\beta_m r_{10}}}{r_{10}}=\frac{1}{2\pi^2}\int d\vec{P}\,\frac{e^{-i\vec{P}\cdot(\vec{r}_1-\vec{r}_0)}}{P^2+\beta_m^2}, \tag{A1}$$

$$\frac{e^{-\beta_n r_{20}}}{r_{20}}=\frac{1}{2\pi^2}\int d\vec{Q}\,\frac{e^{-i\vec{Q}\cdot(\vec{r}_2-\vec{r}_0)}}{Q^2+\beta_n^2} \tag{A2}$$

into the first equality of Eq. (2.15), we obtain

$$\begin{aligned}\mathcal{I}(\vec{q}_0,\gamma,\vec{q}_1,\alpha_i,\vec{q}_2,\alpha_j,\beta_m,\beta_n)&=\frac{1}{64\pi^7}\int d\vec{P}\,\frac{1}{P^2+\beta_m^2}\int d\vec{Q}\,\frac{1}{Q^2+\beta_m^2}\int d\vec{r}_0 d\vec{r}_1 d\vec{r}_2\\&\quad\times\frac{e^{-i(\vec{q}_0+\vec{P}+\vec{Q})\cdot\vec{r}_0-\gamma r_0}}{r_0}\,\frac{e^{-i(\vec{q}_1-\vec{P})\cdot\vec{r}_1-\alpha_i r_1}}{r_1}\,\frac{e^{-i(\vec{q}_2-\vec{Q})\cdot\vec{r}_2-\alpha_j r_2}}{r_2}\\&=\frac{1}{4\pi^3}\int d\vec{Q}\,\frac{1}{Q^2+\beta_m^2}\int d\vec{r}_2\,\frac{e^{-i(\vec{q}_2-\vec{Q})\cdot\vec{r}_2-\alpha_j r_2}}{r_2}\,I(\vec{q}_0+\vec{Q},\gamma,\vec{q}_1,\alpha_i,\beta_m),\end{aligned} \tag{A3}$$

where

$$I(\vec{q}_0+\vec{Q},\gamma,\vec{q}_1,\alpha_i,\beta_m)=\frac{1}{16\pi^4}\int d\vec{r}_0 d\vec{r}_1\,\frac{e^{-i(\vec{q}_0+\vec{Q})\cdot\vec{r}_0-\gamma r_0}}{r_0}\,\frac{e^{-i\vec{q}_1\cdot\vec{r}_1-\alpha_i r_1}}{r_1}\,\frac{e^{-\beta_m r_{10}}}{r_{10}}. \tag{A4}$$

Using Feynman integration technique, it is easy to show that [10]

$$I(\vec{q}_0+\vec{Q},\gamma,\vec{q}_1,\alpha_i,\beta_m)=\frac{1}{\pi^2}\int d\vec{P}\,\frac{1}{(\vec{P}+\vec{q}_0+\vec{Q})^2+\gamma^2}\,\frac{1}{(\vec{P}-\vec{q}_1)^2+\alpha_i^2}\,\frac{1}{P^2+\beta_m^2}=\int_0^1 d\xi\,\frac{1}{\rho_1[(\rho_1+\gamma)^2+(\vec{Q}+\vec{q}_0+\vec{q}_1\xi)^2]}, \tag{A5}$$

where

$$\rho_1=[\beta_m^2+(q_1^2+\alpha_i^2-\beta_m^2)\xi-q_1^2\xi^2]^{1/2}. \tag{A6}$$

Substituting Eq. (A5) into Eq. (A3) and then exchanging the order of integration, we gain

$$\mathcal{I}(\vec{q}_0,\gamma,\vec{q}_1,\alpha_i,\vec{q}_2,\alpha_j,\beta_m,\beta_n)=\int_0^1 d\xi\,\frac{1}{\rho_1}\,\frac{1}{\pi^2}\int d^3Q\,\frac{1}{(\vec{Q}+\vec{q}_0+\vec{q}_1\xi)^2+(\rho_1+\gamma)^2}\,\frac{1}{(\vec{Q}-\vec{q}_2)^2+\alpha_j^2}\,\frac{1}{Q^2+\beta_n^2}$$

$$=\int_0^1 d\xi\,\frac{1}{\rho_1}\,I(\vec{q}_0+\vec{q}_1\xi,\rho_1+\gamma,\vec{q}_2,\alpha_j,\beta_n)$$

$$=\int_0^1 d\xi\,\frac{1}{\rho_1}\int_0^1 d\eta\,\frac{1}{\rho_2[(\rho_2+\rho_1+\gamma)^2+(\vec{q}_0+\vec{q}_1\xi+\vec{q}_2\eta)^2]}$$

$$=\int_0^1 d\xi\int_0^1 d\eta\,\frac{1}{\rho_1\rho_2[(\rho_1+\rho_2+\gamma)^2+q^2]},\tag{A7}$$

where

$$\vec{q}=\vec{q}_0+\vec{q}_1\xi+\vec{q}_2\eta,\tag{A8}$$

$$\rho_2=[\beta_n^2+(q_2^2+\alpha_j^2-\beta_n^2)\eta-q_2^2\eta^2]^{1/2}.\tag{A9}$$

Thus Eq. (2.15) is proved.

[1] M. H. Mittleman, *Introduction to the Theory of Laser-Atom Interactions* (Plenum, New York, 1982).

[2] Claude Cohen-Tannoudji, Jacques Dupont-Roc, and Gilbert Grynberg, *Atom-Photon Interactions: Basic Processes and Applications* (Wiley, New York, 1992).

[3] R. Z. Vitlina, A. V. Chaplik, and M. V. Entin, Sov. Phys. JETP **40**, 829 (1975).

[4] M. H. Mittleman, Phys. Rev. A **14**, 586 (1976).

[5] D. A. Copeland and C. L. Tang, J. Chem. Phys. **66**, 5126 (1977).

[6] Y. P. Hsu, M. Kimura, and R. E. Olson, Phys. Rev. A **31**, 576 (1985).

[7] F. W. Byron, Jr., P. Francken, and C. J. Joachain, J. Phys. B **20**, 5487 (1987).

[8] C. J. Joachain, P. Francken, A. Maquet, P. Martin, and V. Veniard, Phys. Rev. Lett. **61**, 165 (1988).

[9] M. Bhattacharya, C. Sinha, and N. C. Sil, Phys. Rev. A **40**, 567 (1989).

[10] S.-M. Li, Z.-F. Zhou, J.-G. Zhou, and Y.-Y. Liu, Phys. Rev. A **47**, 4960 (1993).

[11] S.-M. Li, J. Chen, J.-G. Zhou, and H.-J. Yin, Phys. Rev. A **47**, 1197 (1993).

[12] C. J. Joachain, *Quantum Collision Theory* (North-Holland, Amsterdam, 1983).

[13] D. Belkić, Phys. Rev. A **47**, 189 (1993).

[14] D. Belkić, Phys. Rev. A **47**, 3824 (1993).

[15] K. H. Berkner, R. V. Pyle, J. W. Sterns, and J. C. Warren, Phys. Rev. **166**, 44 (1968).

[16] E. W. McDaniel, M. R. Flannery, H. W. Ellis, F. L. Eisele, and W. Pole, U.S. Army Missile Research and Development Command Technical Report H, 1977 (unpublished).

[17] L. I. Pivovar, M. T. Novikov, and V. M. Tubaev, Zh. Eksp. Theor. Fiz. **42,** 1490 (1962) [Sov. Phys. JETP **15**, 1035 (1962)].

[18] R. D. Dubois, Phys. Rev. A **36**, 2585 (1987).